Oceanic forcing of the late 20th century Sahel drought

Jian Lu and Thomas L. Delworth

Geophysical Fluid Dynamics Laboratory, NOAA, Princeton, New Jersey, USA

[1]   The Sahel region of Africa underwent a pronounced interdecadal drying trend in the latter half of the 20th century. In order to investigate this drying trend, several ensembles of numerical experiments are conducted using a recently developed atmospheric general circulation model (AM2, developed at NOAA's Geophysical Fluid Dynamics Laboratory). When the model is forced with the time series of observed SSTs and sea ice from 1950 to 2000, it successfully reproduces the observed interdecadal variability of Sahelian rainfall. Additional experiments are used to estimate the separate contributions to Sahel drought from SST anomalies in various ocean basins. In these, SST anomalies are applied only in the tropics, or only in the Atlantic, Indian and Pacific oceans separately. Forcing from the tropical oceans is dominant in driving the Sahelian rainfall trend. The response of Sahel rainfall to a general warming of the tropical oceans suggests a possible link to greenhouse gas-induced climate change.   **Citation:** Lu, J., and T. L. Delworth (2005), Oceanic forcing of the late 20th century Sahel drought, *Geophys. Res. Lett.*, *32*, L22706, doi:10.1029/2005GL023316.

1. Introduction

[2]   The Sahel, a semi-arid area along the southern fringe of the Sahara desert from the Atlantic coast to Ethiopia, underwent a prolonged drought from the late 1960s to the 1990s. This late 20th century drought has been a subject of extensive study [e.g., *Giannini et al.*, 2003; *Ward*, 1998; *Folland et al.*, 1986]. Figure 1 shows the spatial pattern of the linear trend in observed rainfall (data from Climate Research Unit, University of East Anglia) for July–August–September (JAS) over the period 1950 to 2000. The trend of desiccation occurs over the entire Sahel region, with rainfall reductions of 20–50%. Averaging the time series of observed rainfall over the Sahel (defined in this study as 20°W–40°E, 10°N–20°N) gives the Sahel rainfall index (SRI), shown as the red solid line in Figure 1b.

[3]   During the last 30 years, efforts to understand the causes of the drought have been made along two competing directions: "endogenous" vs. "exogenous" [*Brooks*, 2004]. The "endogenous" point of view, pioneered by *Charney* [1975], emphasizes localized feedback between the land degradation/desertification and atmospheric radiation, circulation and precipitation. In contrast, the "exogenous" view looks for forcing of Sahelian changes from processes outside the Sahel, such as the impact of global ocean SST changes [e.g., *Folland et al.*, 1986; *Palmer*, 1986; *Rowell et al.*, 1995].

[4]   Recently, *Giannini et al.* [2003] (hereinafter referred to as G03) successfully simulated the interannual to interdecadal variability of the Sahel rainfall with an atmospheric general circulation model (NSIPP1, developed at NASA's Goddard Space Flight Center) forced by observed SSTs from 1930 to 2000. Their work, in concert with previous studies [e.g., *Palmer*, 1986; *Rowell et al.*, 1995; *Shinoda and Kawamura*, 1994], identified the importance of ocean conditions surrounding Africa in driving the interdecadal trend of the Sahel rainfall. They showed that land-atmosphere interactions amplify the SST-driven signal, but are not instrumental in forcing the drying.

[5]   In G03 the importance of regional SST forcing was deduced based on regression analysis between global SST and Sahelian rainfall. The mechanisms by which the SSTs influence the atmospheric circulation over North Africa, and hence Sahelian precipitation, were not articulated. Thus, following on G03, this study first repeats their experiment using an independent atmospheric general circulation model (described below) driven by observed SSTs from 1950 to 2000. Building from this, the current study uses additional experiments to elucidate the separate roles of the various ocean basins in forcing the Sahelian drying, and diagnoses some of the important physical processes involved.

2. Model and Experiments

[6]   The atmospheric general circulation model employed in this study (AM2) [*Global Atmospheric Model Development Team* (*GAMDT*), 2004] was recently developed at NOAA's Geophysical Fluid Dynamics Laboratory (GFDL). The model has 24 levels in the vertical, with horizontal resolution of 2° latitude by 2.5° longitude. It includes a B-grid atmospheric dynamical core [*Wyman*, 1996], a multi-species three-dimensional aerosol climatology, a fully prognostic cloud scheme and a moist turbulence scheme. The terrestrial component of the model, LM2, is based on the Land Dynamics model described by *Milly and Shmakin* [2002]. The vegetation categories of LM2 are prescribed to be constant on the basis of annual mean observations. Therefore, vegetation feedback is not included in the AM2/LM2 model. For further details see *GAMDT* [2004].

[7]   Several ensembles of experiments are conducted; all ensembles have 10 members, each of which differ in the atmospheric initial states, which are chosen from separate days from a prior integration. First, an ensemble of 51-year experiments from January 1950 to December 2000 is conducted in which the observed time series of SST and sea ice (courtesy of J. Hurrell, NCAR) are prescribed. A similar ensemble is conducted in which observed monthly SST is prescribed only in the tropics (30°S–30°N),
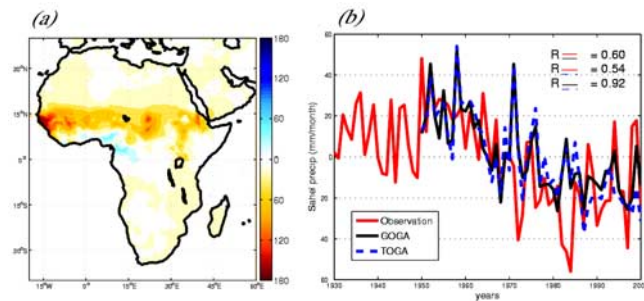
Figure 1. (a) Linear trend of JAS summer precipitation rate from 1950 to 2000 estimated from CRU observations (version CRU-TS_2.1, obtained from the Climate Research Unit at the University of East Anglia). Unit is mm/month/50years. (b) Indices of Sahel rainfall calculated from station data from 1930 to 2000 (red), ensemble mean precipitation rate in GOGA (black solid) and TOGA (dashed) experiments.

otherwise, a climatological seasonal cycle of SST and sea ice is used out of the tropics. We will refer to these two integrations as GOGA and TOGA, respectively.

[8] In order to estimate the role of the different ocean basins in forcing the Sahelian precipitation trend, additional ensembles of experiments are performed. For computational economy, each of the additional experiment runs for 5 months from May 1st to September 30th, with only the JAS output analyzed. As before, ensemble members differ in their atmospheric initial conditions. In the first ensemble (referred to as CONTROL_MS, where the "MS" denotes the May to September duration of individual experiment) the climatological seasonal cycle of SSTs and sea ice is used to force the model. In the second ensemble (referred to as GLOBAL_MS), SST at each ocean grid point is prescribed as the sum of the seasonal cycle plus an anomaly. This anomaly is computed from the linear regression of the time series of observed JAS SST at each grid point versus the low-pass filtered (using 21-year running mean) time series of the observed Sahelian rainfall index. The anomaly SST pattern derived in this manner is shown in Figure 2. The ensemble mean differences for JAS between GLOBAL_MS and CONTROL_MS are used for analysis. A similar strategy has been utilized by *Palmer* [1986] and *Folland et al.* [1986].

[9] Three additional ensembles are conducted, referred to as ATLANTIC_MS, INDIAN_MS, and PACIFIC_MS. They are similar to the GLOBAL_MS case, except that the SST anomalies are added only in the Atlantic, Indian, and Pacific oceans, respectively.

3. Results

[10] The time series of ensemble mean precipitation from GOGA simulation is shown by the solid black line in Figure 1b. The correlation of the simulated SRI time series with the observed index is 0.60, and is 0.3 for the detrended indices, the latter being significant at the 1% level. A similar correlation between the TOGA experiment (shown as dashed line) and the observed SRI indicates that the tropics are the dominant source of SST forcing for the Sahel precipitation variation.

[11] A common feature shared by all three indices is a distinct negative trend from wetter-than-average conditions in the 1950s to drier conditions in the decades of the 1970s and 1980s. Note that the amplitudes of the observed and simulated changes in the SRI are in good agreement. The spatial pattern of the simulated changes (Figure 3a) also compares well with the observations (Figure 1a). The 1990s' recovery of the Sahel rainfall is not well captured by the model, especially in the TOGA simulation.

[12] As documented by observational studies [e.g., *Grist and Nicholson*, 2001; *Fontaine and Janicot*, 1992; *Hastenrath*, 1990] (see also Figure S2[1] for the ERA40 reanalysis results), atmospheric circulation anomalies that accompany the observed Sahelian drought are characterized by the following features relative to the long-term mean: reduced upward motion associated with convection; reduced low-level southwesterly monsoon flow and associated moisture flux near the eastern tropical Atlantic and Guinea Coast; an upper-level tropical Easterly Jet (TEJ, centered at 200 hPa) that is slightly weakened, and does not extend as far south; and a southward displaced African Easterly Jet (AEJ) and associated reduced and displaced wind shear. These features are all reproduced by both the GOGA and TOGA simulations (see Figure S1).

[13] Experiments ATLANTIC_MS, INDIAN_MS, and PACIFIC_MS allow us to estimate the roles of SST anomalies from these respective basins in forcing the Sahelian rainfall changes. We first assess the validity of using the five month experiments, forced with SST anomalies corresponding to the low frequency trend in the Sahel rainfall. This is first shown by comparing Figures 3a and 3b. The GLOBAL_MS experiment simulates a precipitation signal which agrees well with the interdecadal trend simulated in GOGA, although the GLOBAL_MS trend is somewhat larger. In addition, adding the response in ATLANTIC_MS, INDIAN_MS, and PACIFIC_MS largely recovers the response in GLOBAL_MS (Figure 3c). This demonstrates that the use of the ensemble of five month experiments (rather than 50 year experiments) is valid.

[14] The SST forcing pattern used in experiment ATLANTIC_MS (Figure 2) is, in character, an interhemispheric dipole, embedded in which are positive SST anomalies near and to the south of the Equator and negative SST anomalies to the north. The precipitation response to this forcing is also a dipole as shown in Figure 3d. In the tropical Atlantic, the anomalous SST dipolar pattern weakens the climatological northward SST gradient and
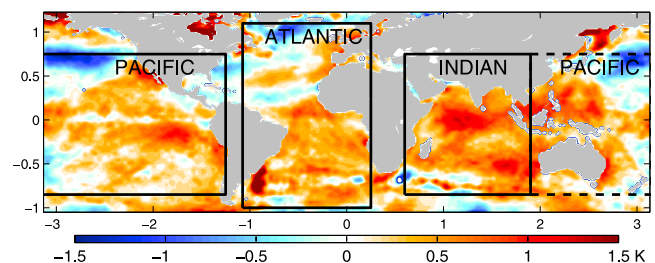

Figure 2. Regression pattern of JAS summer SST during 1950–2000 against the 21-year running mean SRI. The amplitude has been scaled to correspond to the trend during 50 years, with unit of K/50years.
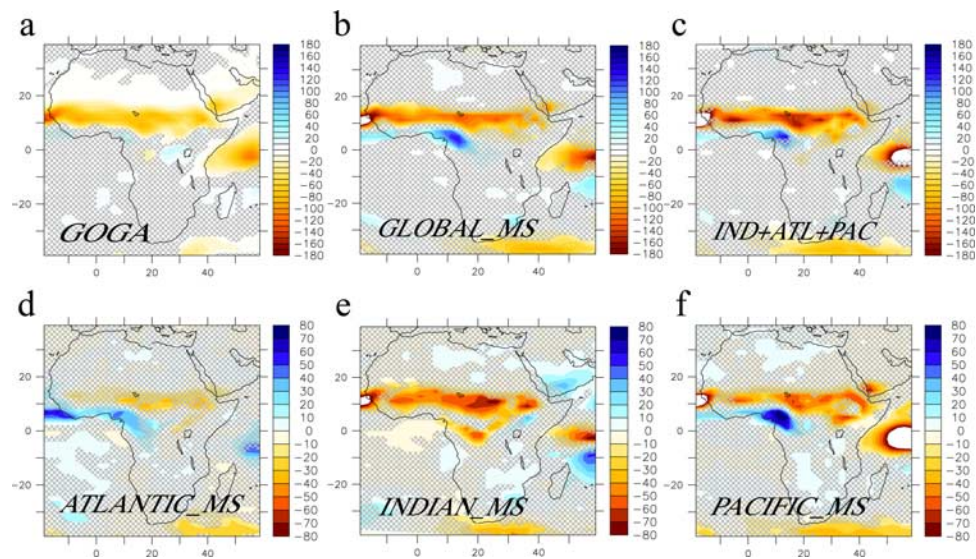

Figure 3. JAS summer mean response of African rainfall to SST forcing in different experiments. For GOGA experiment, plotted is the linear trend of rainfall from 1950–2000. For the other runs, plotted are the differences between the SST anomaly runs and control runs. All the patterns have been scaled to correspond to the trend during 50 years, with unit of mm/month/50years. The hatched areas are not significantly different from zero at 95% level based on t test.

draws the SST and precipitation maxima towards the south. Accordingly, an equatorward displacement takes place in the tropical tropospheric circulation system: near the Guinean coast, the low-level tropospheric wind and moisture convergence are all enhanced; over western tropical Africa, the anomalous zonal wind aloft is characteristic of a meridional dipole, shifting the climatological AEJ southward towards Guinean coast (Figure 4a). Thus, the instability zone of easterly waves associated with the horizontal wind shear at the cyclonic sides of AEJ also shifts southward [*Thorncroft*, 1995; *Thorncroft and Blackburn*, 1999]. In terms of seasonal mean circulation, this is expressed as a slight southward displacement of the rising branch of the Atlantic Hadley cell (Figure 4b). Thus, the shift of rain belt towards the Gulf of Guinea can largely be explained by the shift in the tropical African circulation as a response to the tropical Atlantic SST dipole. On the other hand, the precipitation anomalies over the Sahel in Figure 3d are only marginally different from zero, and are indicative of a weaker sensitivity to the Atlantic SST dipole than that given by *Hoerling et al.* [2005, Figure 8a] and estimated from observations (I. Held et al., Simulations of 20th and 21st century drought in the Sahel, submitted to Proceedings of the National Academy of Sciences, 2005, hereinafter referred to as Held et al., submitted manuscript, 2005). The weak sensitivity to Atlantic SST variations might account for the model's under-representation of the Sahel rainfall recovery during the 1990s, when the Atlantic underwent a progressive warming to the North versus a cooling to the South.

[15] However, the observed changes in the Sahel precipitation are characterized by both a southward displacement of the ITCZ rainbelt and, perhaps to a larger extent, an overall reduction across the whole Sahel region [*Shinoda and Kawamura*, 1994]. In addition, the Atlantic forced rainfall anomalies only account for a fourth of the total Sahel rainfall changes in the GLOBAL_MS experiment.

Thus, oceanic forcing from outside the Atlantic needs to be examined as well.

[16] As shown in Figures 3e and 3f, Indian and Pacific forcing produces relatively stronger aridity over the Sahel. Several features in circulation are commonly shared by the responses to the Indian and Pacific oceanic forcing (see Figure 5): subsidence in the middle troposphere and associated upper tropospheric convergence and lower tropospheric divergence over Sahel region; an anomalous Walker-type overturning cell with ascent from the Indian ocean (for Indian oceanic forcing case) or western Pacific (for Pacific oceanic forcing case) and descent to the Sahel; pairs of cyclonic or anti-cyclonic circulation straddling the equator. These cyclones or anticyclones, symmetric about the equator, are indicative of equatorial Rossby waves as response to the convective heating. The centers of cyclones (anticyclones) match the centers of heating (cooling) in both the Indian and Pacific forced cases, except the latter shifts about 60 degrees in longitude eastward compared to the
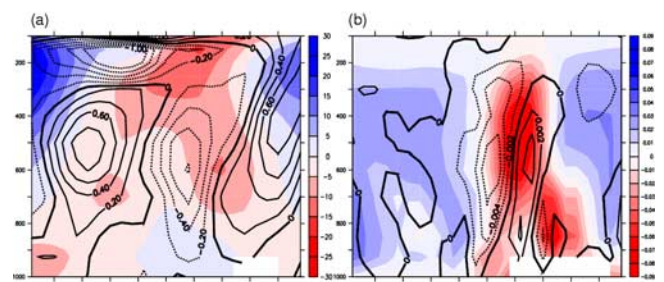

Figure 4. Wind response in ATLANTIC_MS. The anomalies are plotted as contours overlaying the corresponding climatology as color-shading background. (a) Zonal wind averaged between 20°W and 25°E. (b) Vertical velocity (omega, Pa/s) averaged between 20°W and 25°E.
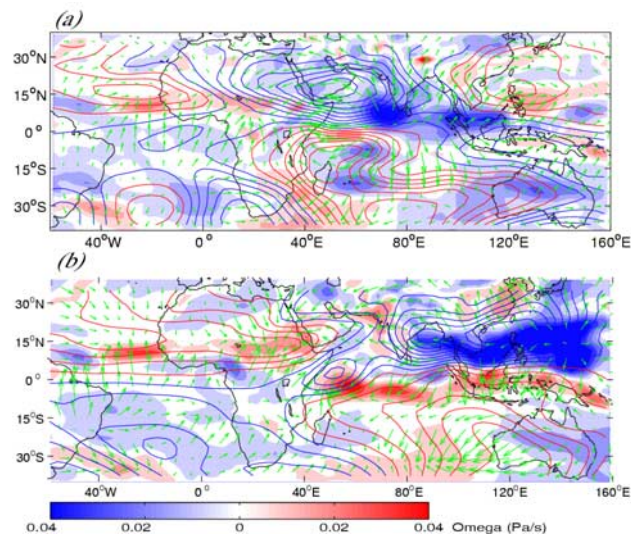
Figure 5. (a) 700 hPa eddy streamfunction (contours, blue for negative and red for positive isopleths), 500 hPa vertical velocity (omega, color shading) and 300 hPa divergent wind (arrows) in INDIAN_MS. (b) Same as Figure 5a except for PACIFIC_MS.

former. However, the Sahelian subsidence undergoes little shift between these two cases. As such, the rotational component of the response can be largely interpreted as a Gill-type [*Gill*, 1980] stationary Rossby wave solution to the heating induced by tropical SST warming. The reasons for the insensitivity of the Sahel rainfall response to the location of the heating are not well understood.

4. Summary and Discussion

[17] Experiments are conducted with GFDL's AM2 atmospheric general circulation model to investigate the mechanisms of the decreasing trend of Sahel rainfall in the second half of the 20th century. Results show that when the model is forced with observed SSTs it can quite realistically reproduce the spatial pattern and amplitude of the observed Sahelian drying. Further, while all tropical ocean basins appear to contribute to the Sahelian drying, SST changes in the Indian and Pacific basins have a greater impact than Atlantic SST changes. Such a result could well be model dependent. For instance, using a variety of models and driving these models with the observed Indian or Atlantic SST variations alone, *Hoerling et al.* [2005] found that the impact of Indian Ocean warming is a drying (wetting) in the southern (northern) part of the Sahel, resulting in little net precipitation change over the Sahel. In contrast, the precipitation anomalies forced by the Atlantic SST projects strongly upon the pattern of the observed rainfall trend over north Africa. Using a different model (ECHAM4.5), J. Bader and M. Latif (Combined tropical oceans drive anomalous sub-Saharan west African rainfall, submitted to *Journal of Climate,* 2005) found a drying over western Subsaharan Africa in response to a 1K increase in Indian Ocean SSTs. This divergence of modeling results suggests that additional investigation is required to more confidently assess the relative roles of the various tropical oceans in forcing the Sahelian drought.

[18] If the warming over the Indian and Pacific oceans is the major source of the Sahel drying trend, one may naturally wonder to what extent this is related to anthropogenic climate change, particularly in light of several studies that have suggested that the observed Indian ocean warming reflects anthropogenic forcing [*Knutson et al.*, 1999; *Hurrell et al.*, 2004]. A wide range of numerical experiments using a coupled model at GFDL, whose atmospheric component is AM2, have recently been completed (see *Delworth et al.* [2005] for a description of the coupled model). For simulations of the 20th century, in which the model is forced with observational estimates of changes in greenhouse gases, aerosols, volcanic forcing, solar forcing, and land use, the models simulated a drying trend over the Sahel in the second half of the 20th century, with an amplitude approximately 50% of the observed trend. In addition, simulations of the 21st century using this model, as well as additional experiments using idealized increases of CO_2, all simulate a further drying of the Sahel in response to general warming. Detailed analysis of these coupled model experiments will be reported in a separate paper (Held et al., submitted manuscript, 2005). These coupled model results suggest that a CO_2 induced global SST increase does play a part in the Sahel drought, at least in the context of the GFDL coupled climate model.

References

Brooks, N. (2004), Drought in the African Sahel: Long term perspectives and future prospects, *Tyndall Cent. Working Pap. 61*, University of East Anglia, Norwich, U. K.

Charney, J. G. (1975), Dynamics of deserts and drought in the Sahel, *Q. J. R. Meteorol. Soc., 101*, 193–202.

Delworth, T. L., et al. (2005), GFDL's CM2 global coupled climate models-part 1: Formulation and simulation characteristics, *J. Clim.*, in press.

Folland, C. K., T. N. Palmer, and D. E. Parker (1986), Sahel rainfall variability and worldwide sea temperature, 1901–85, *Nature, 320*, 602–606.

Fontaine, B., and S. Janicot (1992), Wind-field coherence and its variations over west Africa, *J. Clim., 5*, 512–524.

Giannini, A., R. Saravanan, and P. Chang (2003), Oceanic forcing of Sahel rainfall on interannual and to interdecadal time scales, *Science, 302*, 1027–1030.

Gill, A. E. (1980), Some simple solutions for heat-induced tropical circulation, *Q. J. R. Meteorol. Soc., 106*, 447–462.

Global Atmospheric Model Development Team (GAMDT), (2004), The new GFDL global atmospheric and land model AM2/LM2: Evaluation with prescribed SST simulations, *J. Clim., 17*, 4641–4673.

Grist, J. P., and S. E. Nicholson (2001), A study of dynamics factors influencing the rainfall variability in the west African Sahel, *J. Clim., 14*, 1337–1359.

Hastenrath, S. (1990), Decadal-scale changes of the circulation in the tropical Atlantic sector associated with Sahel drought, *Int. J. Climatol., 10*, 459–472.

Hoerling, M. P., J. W. Hurrell, and J. Eischeid (2005), Impact of greenhouse warming on the West African summer monsoon, *J. Clim.*, in press.

Hurrell, J. W., M. P. Hoerling, A. S. Phillips, and T. Xu (2004), Twentieth century North Atlantic climate change. Part I: Assessing determinism, *Clim. Dyn., 23*, 371–389.

Knutson, T. R., T. L. Delworth, K. W. Dixon, and R. J. Stouffer (1999), Model assessment of regional surface temperature trends (1949–1997), *J. Geophys. Res., 104*, 30,981–30,996.

Milly, P. C. D., and A. B. Shmakin (2002), Global modeling of land water and energy balances. Part I: The land dynamics (LaD) model, *J. Hydrometeorol., 3*, 283–299.

Palmer, T. N. (1986), Influence of the Atlantic, Pacific and Indian Oceans on Sahel rainfall, *Nature, 320*, 251–253.

Rowell, D. P., C. K. Folland, K. Maskell, and M. N. Ward (1995), Variability of summer rainfall over tropical north Africa (1906–92): Observations and modeling, *Q. J. R. Meteorol. Soc.*, *121*, 669–704.

Shinoda, M., and R. Kawamura (1994), Tropical rainbelt, circulation, and sea surface temperatures associated with the Sahelian rainfall trend, *J. Meteorol. Soc. Jpn.*, *72*, 341–357.

Thorncroft, C. D. (1995), An idealized study of African easterly waves. III: More realistic basic states, *Q. J. R. Meteorol. Soc.*, *121*, 1589–1614.

Thorncroft, C. D., and M. Blackburn (1999), Maintenance of the African easterly jet, *Q. J. R. Meteorol. Soc.*, *125*, 763–786.

Ward, M. N. (1998), Diagnosis and short-lead time prediction of summer rainfall in tropical north Africa at interannual and interdecadal timescales, *J. Clim.*, *11*, 3167–3191.

Wyman, B. L. (1996), A step-mountain coordinate general circulation model: Description and validation of medium-range forecasts, *Mon. Weather Rev.*, *124*, 102–121.

T. L. Delworth and J. Lu, Climate Dynamics and Prediction Group, Geophysical Fluid Dynamics Lab, NOAA, Forrestal Campus, P. O. Box 308, US Route 1 North, Princeton, NJ 08540, USA. (jian.lu@noaa.gov)